C S S A

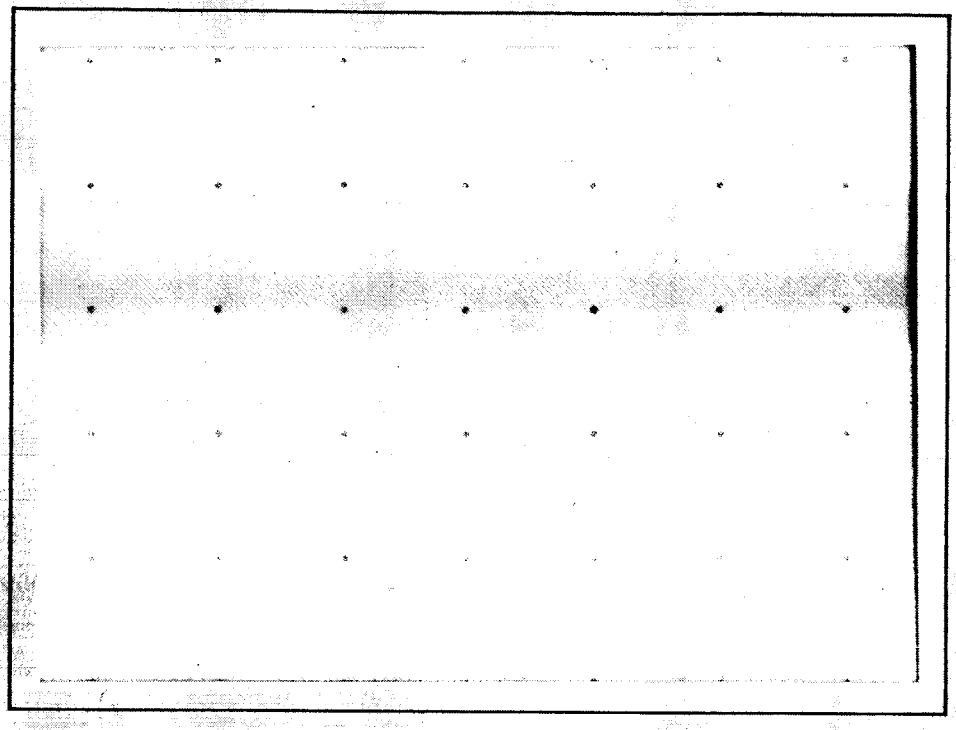

CENTER FOR SPACE SCIENCE AND ASTROPHYSICS
STANFORD UNIVERSITY
Stanford, California

RAPID TEMPORAL EVOLUTION OF RADIATION FROM NON-THERMAL ELECTRONS IN SOLAR FLARES

EDWARD T. LU[1]

AND

VAHÉ PETROSIAN[1]

CSSA-ASTRO-87-5

June 1987

[1]Department of Applied Physics, Stanford University

National Aeronautics and Space Administration Grant NSG 7092

National Science Foundation Grant ATM 8320439

ABSTRACT

We have found analytic solutions of the time dependent Fokker-Planck equation for accelerated electrons undergoing Coulomb collisions in a magnetized, fully ionized plasma. First we find an exact solution for arbitrary pitch angle and energy distribution in a uniform background plasma. Then, for an inhomogeneous plasma we find an approximate solution for particles with small pitch angles. We have used these solutions to calculate the temporal evolution of bremsstrahlung x-rays from short bursts of non-thermal electron beams, and compared these spectra with observed high time resolution spectra of short timescale solar hard x-ray bursts. We show that, as expected, the observed softening in time of the spectra rules out a homogeneous background and therefore the possibility of electrons being confined to the corona either because of converging magnetic field or high densities. We also apply the inhomogeneous solution to a model with constant coronal density and exponentially rising chromospheric density. The spectra are shown to be consistent with that produced by a collimated beam of electrons accelerated in the corona with the following restrictions: the electrons must be injected over a time t_0 with $.1\,\mathrm{s} \lesssim t_0 \lesssim .2\,\mathrm{s}$; the coronal loop length must be longer than $\sim 5 \times 10^8$ cm (which rules out acceleration near or below the transition region); the scale height below the transition region must be shorter than $\sim 3 \times 10^8$ cm; the column depth above the transition must be less than $1.7 \times 10^{20}\,\mathrm{cm}^{-2}$; and depending on the collimation of the beam the magnetic field must not converge rapidly. These conditions could violated if large pitch angle electrons are present.

RAPID TEMPORAL EVOLUTION OF RADIATION FROM NON-THERMAL ELECTRONS IN SOLAR FLARES

I. INTRODUCTION

It is generally agreed that the bulk of the hard x-ray emission from the impulsive phase of solar flares is due to thick target bremsstrahlung emission from non-thermal electrons. In these models, electrons are accelerated in the corona and stream downwards along magnetic field lines towards the chromosphere where they lose most of there energy through Coulomb collisions with the background plasma particles. Until recently, the time resolution of observing instruments has been longer than the typical interaction timescale of the electrons. Short timescale variations were therefore lost in the time integration of the instruments. Consequently, most of the calculations of x-ray spectra have assumed steady state conditions (e.g. Brown 1973, Leach and Petrosian 1983). However, observations from the hard x-ray burst spectrometer (HXRBS) on SMM have provided high time resolution spectral information on hard x-ray bursts (Kiplinger et al 1983). Figure 1 shows an example of a burst with a rise time of $\sim$ .25 s and a decay time of $\sim$ .4 s reported by Kiplinger et al (1984). Over the course of a burst, the spectra show gradual softening on timescales of a tenths of a second and shorter (Kiplinger et al 1984, see also Kane and Anderson 1970). Since this time is of the order of the collisional timescale for particles, steady state treatments of the problem are not valid. Emslie (1983) considered the time dependent problem but did not include the full effect of scattering on the distribution of electrons. We will solve the time dependent Fokker-Planck equation including both energy loss and pitch angle diffusion for electrons stopped in a background plasma. In section II we present

analytic solutions for the case when the background plasma is of constant density, and for the case when the background plasma density is spatially varying but the electrons are moving with small pitch angles with respect to the magnetic field. In section III we assume a model for the x-ray burst region and use the solutions developed in section II to calculate the bremsstrahlung x-ray spectra produced as a function of time. We then compare these time dependent x-ray spectra to the observations, and from this place constraints on the length of the coronal magnetic loops and on the characteristics of the initial injection spectrum of the electrons. Section IV provides a summary.

II. THE TIME DEPENDENT KINETIC EQUATION

The Fokker-Planck equation describing the evolution of a distribution $f(E, \mu, s, t)$ of electrons injected into a cold ionized hydrogen plasma with a magnetic field of strength B is

$$\frac{\lambda_0}{c\beta}\frac{\partial f}{\partial t} + \lambda_0 \mu \frac{\partial f}{\partial s} = \lambda_0 \frac{(1-\mu^2)}{2}\frac{dlnB}{ds}\frac{\partial f}{\partial \mu} + \frac{1}{\beta}\frac{\partial}{\partial E}(\frac{f}{\beta}) + \frac{1}{\beta^4\gamma^2}\frac{\partial}{\partial \mu}[(1-\mu^2)\frac{\partial f}{\partial \mu}]. \quad (1)$$

This is an extension of the steady state Fokker-Planck equation derived in Leach and Petrosian (1983) to which we have added the time evolution term $(\lambda_0/c\beta)\partial f/\partial t$.

The length scale $\lambda_0 \equiv (10^{24}\,\mathrm{cm})(n_e/\,\mathrm{cm}^{-3})^{-1}(\ln\Lambda)^{-1}$, where n_e is the background electron number density and $\ln\Lambda \approx 20$ is the Coulomb logarithm. Note that λ_0 is in general a function of the spatial coordinate s. The remaining variables are as defined in Leach and Petrosian (1983) with μ being the cosine of the pitch angle with respect to the magnetic field, and $E = \gamma - 1$ being the kinetic energy in units of $m_e c^2$. It is convenient to define the dimensionless column depth τ as $d\tau \equiv ds/\lambda_0 \equiv nds/N_0$, where

$N_0 = (10^{24}\,\mathrm{cm}^{-2})(\ln\Lambda)^{-1}$. This is a one spatial dimensional problem as the electrons are assumed to be tied to the field lines so that diffusion across the field lines can be ignored.

From a given distribution $f(E,\mu,s,t)$, it is a straightforward matter to evaluate the bremsstrahlung spectrum $I(k,\theta,s,t)$ as a function of the angle of emission θ with respect to the local magnetic field, and the photon energy k at each space and time point. However, the high time resolution x-ray observations are spatially unresolved and thus correspond to the x-ray flux integrated over the entire emission region, which we assume to be a closed magnetic loop. The spatially integrated x-ray spectrum in a direction Θ with respect to some fixed axis (such as the earth-sun axis) is then

$$I(k,t,\Theta) = \int_k^\infty dE \int_{-1}^1 d\mu \int_{-\infty}^\infty n\beta f(E,\mu,t,s)\sigma(k,\Theta,E,\mu)ds. \tag{2}$$

In general, because of the complicated geometry of the flaring loop, the angles θ, Θ, and μ are related in a complicated manner which is a function of position. At low energies (k, $E \ll 1$), σ is nearly isotropic so we can take σ out of the integrals over s and μ. As k and E increase, this approximation becomes less and less valid. However, at higher energies most of the emission will come from deeper regions of the chromosphere where the magnetic field is approximately straight. In this case Θ is independent of s so we can again take σ out of the integral over s. Then if we define an integrated electron flux

$$F(E,t,\mu) \equiv \int_{-\infty}^\infty \beta f(E,\mu,s,t)d\tau = \frac{1}{N_0}\int_{-\infty}^\infty \beta f(E,\mu,s,t)n(s)ds, \tag{3}$$

equation (2) becomes

$$I(k,t,\Theta) = N_0 \int_k^\infty dE \int_{-1}^1 d\mu F(E,\mu,t)\sigma(k,\Theta,E,\mu). \tag{4}$$

If we integrate equation (4) over all directions of emission we obtain the total spectrum as a function of time.

$$I(k,t) = N_0 \int_0^\infty G(E,t)\sigma(k,E)dE \tag{5}$$

$$G(E,t) \equiv \int_{-1}^{1} F(E,\mu,t)d\mu \tag{6}$$

Here $\sigma(k,E)$ is the integrated (over angles) bremsstrahlung cross section for emission of photons of energy k by electrons of energy E. For non-relativistic energies the Bethe-Heitler cross section is used.

$$\sigma(k,E) \propto \frac{1}{kE}\ln\left(\frac{1+(1-k/E)^{1/2}}{1-(1-k/E)^{1/2}}\right) \tag{7}$$

The spectrum in a particular direction may, however, be different than the total spectrum. In general for energies below 100 keV we expect the difference to be small (Petrosian 1973), especially if we consider the effect of the photospheric albedo (Bai and Ramaty 1978, Langer and Petrosian 1977) which tends to isotropize the emission. More importantly however, the time evolution of both the mean and directional spectra will be similar so that $I(k,t)$ will give us a good representation of the temporal evolution of the emission in a particular direction. For the purposes of this paper we are primarily concerned with the temporal evolution of the x-ray spectrum. A more detailed analysis would have to take into account the anisotropic emission, the photospheric albedo, and the geometry of the loop. Furthermore, we neglect the effects of plasma wave generation by the electron beam which could make the spectral time variations we will consider less pronounced.

With the approximations of equations (5) and (7) it can be shown that the logarithmic part of equation (7) has negligible effect on the spectra at the level of the existing

observations (Petrosian 1973). In this case a power law integrated flux $F(E) \propto E^{-\delta}$ will lead to a power law x-ray spectrum $I(k) \propto k^{-\delta-1}$. As we shall see, for an electron injection spectrum which is a power law, the integrated electron flux $G(E,t)$ will be an approximate power law so that the approximation $I(k,t) \propto G(k,t)/k$ is valid. Consequently, we shall use the electron spectrum $G(E,t)$ to distinguish between models. We have however tested the validity of this approximation by integrating equation (5) and found it to be within the accuracy needed for this analysis.

In other astrophysical situations, however, and for higher spatial and spectral resolution, knowledge of the spatial and angular dependance of the distribution function may be required. We therefore present first some general solutions explicitly showing the spatial and angular dependence of the electron distribution.

A. Homogeneous Case

i) General Solution: Here we assume the plasma density and magnetic field are constant so that λ_0 is constant and $d\ln B/ds = 0$. It is then useful to define the dimensionless time variable y,

$$y \equiv \frac{ct}{\lambda_0} \equiv \frac{t}{T}. \tag{8}$$

Integrating equation (1) over τ and making use of the fact that there are no particles at $\tau = \pm\infty$ we obtain

$$\frac{\partial F}{\partial y} = \frac{\partial}{\partial E}\left(\frac{F}{\beta^2}\right) + \frac{1}{\beta^3\gamma^2}\frac{\partial}{\partial \mu}\left[(1-\mu^2)\frac{\partial F}{\partial \mu}\right]. \tag{9}$$

This equation also describes the situation where the same distribution of electrons is injected throughout an infinite and homogeneous plasma.

Defining new variables $\phi \equiv F/\beta^2$, $d\tilde{\eta} \equiv \beta dE$, and $d\rho/d\tilde{\eta} \equiv 1/\beta^3\gamma^2$ so that

$$\tilde{\eta} = (E^2 + 2E)^{\frac{1}{2}} + \sin^{-1}\Big(\frac{1}{E+1}\Big), \tag{10}$$

and

$$\rho = \frac{1}{2}\ln\Big(\frac{E}{E+2}\Big), \tag{11}$$

equation (9) becomes

$$\frac{\partial\phi}{\partial y}\frac{\partial\tilde{\eta}}{\partial\rho} - \frac{\partial\phi}{\partial\rho} = \frac{\partial}{\partial\mu}[(1-\mu^2)\frac{\partial\phi}{\partial\mu}]. \tag{12}$$

The distribution ϕ is now separable and can be written in the form

$$\phi(\tilde{\eta},\mu,y) = \sum_{l=0}^{\infty} e^{l(l+1)\rho(\tilde{\eta})}\, Z_l(y+\tilde{\eta})P_l(\mu), \tag{13}$$

where $P_l(\mu)$ are the Legendre polynomials, and $Z_l(y+\tilde{\eta})$ are functions to be determined from the boundary condition of the distribution of electrons at injection.

In what follows we shall assume that the initial injected electron flux is separable in pitch angle, energy, and time.

$$F(\tilde{\eta},\mu,y) = g(\tilde{\eta})h(\mu)k(y) \tag{14}$$

It is convenient to find the solution for a delta function injection time profile $k(y) = \delta(y)$ which we designate by $F_\delta(\tilde{\eta},\mu,y)$. The general solution for an arbitrary injection time profile $k(y)$ is found by convolving the solution for a delta function injection with $k(y)$

$$F(E,\mu,t) = \int_{-\infty}^{y} k(y')F_\delta(y-y')dy'. \tag{15}$$

Evaluating equation (13) at $y = 0$ and using the orthogonality of the $P_l(\mu)$ we obtain

$$Z_l(\tilde{\eta}) = \frac{2l+1}{2}e^{-l(l+1)\rho(\tilde{\eta})}\,\frac{g(\tilde{\eta})}{\beta^2(\tilde{\eta})}\int_{-1}^{1} P_l(\mu')h(\mu')d\mu'. \tag{16}$$

Inserting $Z_l(\tilde{\eta}+y)$ back into equation (13) gives

$$F_\delta(t,E,\mu)=\frac{\beta^2(\tilde{\eta})}{\beta^2(\tilde{\eta}+y)}g(\tilde{\eta}+y)\sum_{l=0}^{\infty}\frac{2l+1}{2}\left[\int_{-1}^{1}P_l(\mu')h(\mu')d\mu'\right]e^{-l(l+1)[\rho(\tilde{\eta}+y)-\rho(\tilde{\eta})]}\,P_l(\mu) \tag{17}$$

for the distribution of the flux of electrons as a function of time after the electrons are injected at $y=0$.

Note that the factor

$$e^{-l(l+1)[\rho(\tilde{\eta}+y)-\rho(\tilde{\eta})]}=\left[\left(\frac{E(\tilde{\eta}+y)}{E(\tilde{\eta})}\right)\left(\frac{E(\tilde{\eta})+2}{E(\tilde{\eta}+y)+2}\right)\right]^{-l(l+1)/2}$$

decreases rapidly with increasing l and time y so that only a limited number of terms need be considered in the sum as y increases.

As is evident, the distribution scales with time as $\tilde{\eta}+y$. In general, $g(\tilde{\eta})$ will be a rapidly decreasing function of $\tilde{\eta}$ such as a power law in energy. We can therefore identify $y=\tilde{\eta}$ as the stopping time for electrons of energy parameter $\tilde{\eta}$. For non-relativistic particles, $\tilde{\eta}\approx E^{3/2}$, so the stopping time will be proportional to $E^{3/2}$. This is as expected since the scattering cross section decreases as E^{-2} while the rate at which the electron travels through the plasma increases as $E^{1/2}$.

ii) The Small Pitch Angle Solution: In the limit of small pitch angle (electrons moving approximately parallel to the field lines, $\mu\approx 1$), the solution can be expressed in a more manageable form which involves an integral instead of an infinite series. This integral can be performed in closed form in certain cases. In addition, this solution can be extended to the inhomogeneous (τ dependent) case as described in the next part.

Let α be the sine of the pitch angle

$$\alpha\equiv(1-\mu^2)^{\frac{1}{2}}\approx\text{pitch angle}\ll 1 \tag{18}$$

To first order in α equation (9) becomes

$$\frac{\partial F}{\partial y} = \frac{\partial}{\partial E}(\frac{F}{\beta^2}) + \frac{1}{\beta^3\gamma^2}\frac{1}{\alpha}\frac{\partial}{\partial \alpha}(\alpha\frac{\partial F}{\partial \alpha}) \tag{19}$$

which can be solved as was equation (9) to yield

$$F_\delta(t,E,\mu) = \frac{\beta^2(\tilde{\eta})}{\beta^2(\tilde{\eta}+y)} g(\tilde{\eta}+y)\times \int_0^\infty e^{-\omega^2[\rho(\tilde{\eta}+y)-\rho(\tilde{\eta})]}\left[\int_0^\infty J_0(\omega\alpha')h(\alpha')\alpha' d\alpha'\right] J_0(\omega\alpha)\omega d\omega. \tag{20}$$

This solution is similar to the spatially homogeneous but time independent solution of equation (1) (cf. Leach and Petrosian 1983). For an initial distribution which is gaussian in α,

$$h(\alpha) = (\frac{2}{\alpha_0^2})e^{-\alpha^2/\alpha_0^2}, \tag{21}$$

the integrals in equation (20) can be solved to yield a pitch angle distribution which remains gaussian, but with a dispersion which increases in time.

$$F_\delta(t,E,\mu) = \frac{\beta^2(\tilde{\eta})}{\beta^2(\tilde{\eta}+y)} g(\tilde{\eta}+y)\Big(\frac{2}{\alpha_t^2}\Big)e^{\frac{-\alpha^2}{\alpha_t^2}}. \tag{22}$$

$$\alpha_t^2 \equiv \alpha_0^2 + 4[\rho(\tilde{\eta}+y) - \rho(\tilde{\eta})] \tag{23}$$

The small pitch angle approximation breaks down at non-relativistic energies for times $y \gtrsim E^{3/2}$ since electrons of energy E are scattered away from the small pitch angle regime in time of order $y \approx E^{3/2}$. We have compared the exact solution (17) and the approximate solution (22) for a gaussian pitch angle injection with $\alpha_0^2 \ll 1$. We find them to agree well ($\sim 20\%$), for $\alpha \lesssim .2$, and for $y \lesssim E^{3/2}$ when the summation of Legendre Polynomials in equation (17) was truncated at $l = 12$.

The integration over μ of the exact solution equation (17) (or the solution (22)) is trivial and replaces the series in (17) (or the last two terms in (22)) with unity. Substituting this into equation (15) we obtain the general integrated time dependent electron spectrum $G(E,t)$ needed for the calculation of the bremsstrahlung spectrum.

$$G(E,t) = \int_{-\infty}^{y} \frac{\beta^2(\tilde{\eta})}{\beta^2(\tilde{\eta}+y-y')} g(\tilde{\eta}+y-y')k(y')dy' \tag{24}$$

This result can also be obtained directly by noting that integration of equation (12) over $d\mu$ gives zero on the right hand side. Solving the resulting equation gives equation (24).

B. Inhomogeneous Case

It turns out that a method similar to that used for the homogeneous case in the small pitch angle regime yields a solution (albeit a a complicated one) for the spatially inhomogeneous case. This solution includes the effects of spatial variation of the background density and magnetic field (for a distribution integrated over pitch angle). The general solution is discussed in detail in the Appendix. Here we assume $d\ln B/ds = 0$. Since λ_0 (or T) is now a function of τ, we no longer use the variable y. Making the T dependence explicit, the equation to be solved is

$$\frac{T(\tau)}{\beta}\frac{\partial f}{\partial t} + \frac{\partial f}{\partial \tau} = \frac{1}{\beta}\frac{\partial}{\partial E}\left(\frac{f}{\beta}\right) + \frac{1}{\beta^4\gamma^2}\frac{1}{\alpha}\frac{\partial}{\partial \alpha}\left(\alpha\frac{\partial f}{\partial \alpha}\right). \tag{25}$$

The general solution of this equation is presented in the Appendix. For an initial particle flux distribution at $\tau = 0$ of $F(E,\alpha,\tau=0,t) = g(E)h(\alpha)k(t)$, this has the solution (see equation A26)

$$F(E,\mu,\tau,t) = \frac{\beta^2(\eta)}{\beta 2(\eta+\tau)} g(\eta+\tau)k\Big(t-\Omega(\eta,\tau)\Big)\int_0^\infty e^{-\omega^2[\rho(\eta+\tau)-\rho(\eta)]}\, H(\omega)J_0(\omega\alpha)\omega d\omega, \tag{26}$$

where

$$\eta \equiv \int \beta^2 dE = \frac{E^2}{E+1}, \tag{27}$$

$$\Omega(\eta,\tau) \equiv \int_0^s \frac{ds'}{c\beta(\eta+\tau-\tau(s'))}, \tag{28}$$

$$H(\omega) \equiv \int_0^\infty J_0(\omega\alpha)h(\alpha)\alpha d\alpha, \tag{29}$$

and $\rho(\eta)$ is as defined in equation (11). For $h(\alpha)$ a gaussian as in equation (21) the integral over ω can be performed to yield

$$F(E,\mu,\tau,t) = \frac{\beta^2(\eta)}{\beta^2(\eta+\tau)} g(\eta+\tau)k\Big(t-\Omega(\eta,\tau)\Big)\Big(\frac{2}{\alpha_t^2}\Big)e^{\left(\frac{-\alpha^2}{\alpha_t^2}\right)}. \tag{30}$$

The function $\Omega(\eta,\tau)$ has the simple physical interpretation of being the the time it takes for an electron having energy $E(\eta+\tau-\tau(s'))$ at s' to travel a distance s. This electron has energy E at s but started out with energy $E(\eta+\tau)$ at $s=0$. Thus, the whole distribution scales with energy as $E(\eta+\tau)$. However, since the Fokker-Planck equation is a statistical equation and does not follow individual electrons, this does not describe what actually happens to a single electron but rather what happens to the distribution. For extremely relativistic particles, $\beta \approx 1$, this integral reduces to

$$\Omega(\eta,\tau) = \int_0^s \frac{ds'}{c} = \frac{s}{c}. \tag{31}$$

Thus the solution has a time dependence $k(t-s/c)$ which means that the distribution propogates along the field lines with velocity c. This is just what is expected for small pitch angle relativistic particles. We caution here that for extremely relativistic particles the equation used by Leach (1984) and here for the small pitch angle regime needs corrections (McTiernan and Petrosian 1987).

The function $\Omega(\eta, \tau)$ can also be expressed in closed form for the case of constant background density T=constant. The time dependence will then be of the form

$$k(t - (\lambda_0/c)[\tilde{\eta}(\eta + \tau) - \tilde{\eta}(\eta)]). \tag{32}$$

where $\tilde{\eta}(\eta)$ is the function $\tilde{\eta}$ defined in equation (10) written as a function of η defined in equation (27). This assertion can be readily proven by inserting equation (35) into equation (25). Note that just as for the homogeneous case the flux integrated over pitch angle can be carried out trivially. As shown in the Appendix, this is also possible for the case with non-uniform magnetic field as long as the pitch angle remains small. The spatial integration, however, cannot be done analytically.

III. NUMERICAL RESULTS AND COMPARISON WITH OBSERVATIONS

Here we present the variation in time of the x-ray spectrum assuming that the injected electron flux is a separable function of time, pitch angle, and energy as in equation (14). Furthermore, as described at the end of section I, for the purposes of this paper we need only to consider the spatially and angularly integrated electron spectrum $G(E, t)$.

Figure 2 shows G(E,t) for the constant density case (equation 24), for a gaussian injection time profile $k(t) = \exp(-t^2/t_0^2)$, and an initial energy spectrum which is a power law $g(E) \propto E^{-\delta}$. The important thing to note about this figure is that the spectrum hardens in time. As was pointed out by previous authors (Kane and Anderson 1970, Petrosian 1973), spectral hardening is expected in a constant density background because the stopping time for non-relativistic electrons is proportional to $E^{3/2}$. Again, this assumes the injected electron energy spectrum does not change in time. Since the function $G(E, t)$

becomes flatter in time, we can immediately conclude that the electrons are not collisionally stopped in the constant density corona. If there is no appreciable magnetic mirroring which traps the electrons in the corona so that the majority of electrons only traverse down the loop once, then an upper limit can be placed on the integrated column density of the loop in the corona from the acceleration region to the transition region, N_{tr}. The absence of hardening in the spectrum shown in figure 3 shows that most of the electrons with $E \gtrsim .06$ (i.e. $\gtrsim 30$ KeV) go through the corona and enter the chromosphere. Thus $\tau_{tr} < \eta(E = .06) = 3.4 \times 10^{-3}$

$$N_{tr} \equiv \int_{corona} nds < 1.7 \times 10^{20} \mathrm{cm}^{-2} \tag{33}$$

For a coronal density $n = 10^{10} \mathrm{cm}^{-3}$, this constrains the coronal loop length to be less than 1.7×10^{10}cm (not a very stringent limit).

This observation also places a limit on the convergence of the magnetic field, $d\ln B/d\tau$. This is because a converging field will trap electrons in the uniform density corona and produce x-ray spectra which harden in time. Just how small $d\ln B/d\tau$ must be depends on the pitch angle distribution since the smaller the pitch angles, the greater must be the magnetic convergence to trap the particles. Our analytic solution assumes constant B field so that for a quantitative limit on $d\ln B/ds$, one needs numerical solutions of the Fokker-Planck equation. However, neglecting collisions in the low density coronal portion of the loop, we can estimate that the ratio of the field at the transition region to that at the injection region $(B_{tr}/B_{inj}) < \alpha_0^{-2}$.

Another argument against the electrons being stopped in the corona is that the decay time of the burst is too long for reasonable values of density. In order to produce a burst

decay time of order a few tenths of a second in a uniform background, the background density must exceed 10^{12} cm^{-3}. This would be an extremely high coronal density. In any case, this would also produce a spectrum which hardens markedly over the course of the burst, contrary to the observations.

It is possible to produce a spectrum which softens in time with a background density which increases with distance from the injection point. This is because the higher energy electrons penetrate to the denser plasma faster and can thus decay faster than the lower energy electrons (cf Petrosian 1973). This condition requires the solution of the inhomogeneous equation. We can analyze this situation if the injected electrons have small pitch angles. The x-ray spectral evolution was calculated using equation (30) for a model where the input spectrum integrated over pitch angles was

$$F(E, s = 0, t) = E^{-\delta} \exp(-t^2/t_0^2) \tag{34}$$

The density n was

$$n = \begin{cases} n_0 & 0 < s < s_t \\ n_0 \exp(s/s_0) & s > s_t \end{cases} \tag{35}$$

with s_t the half length of the loop above the transition region and s_0 the scale height below the transition region. Figure 3 shows the spectral evolution of $G(k,t)/k$ for $n_0 = 10^{10}$ cm^{-3}, $s_0 = 10^7$ cm, $s_t = 1.4 \times 10^9$ cm, $\delta = 4.2$, and $t_0 = .13$ sec. For comparison, measured spectra from the HXRBS (from Kiplinger et al 1984) are also plotted on the same graphs. The calculated spectra are time integrated over 128 ms intervals in order to match the time resolution of the HXRBS.

The value of n_0 does not have much effect on the spectra because s_t and n_0 are chosen so that few electrons are stopped in the corona, $\tau(s_t) \ll \eta$. We also find that the degree

of spectral softening is not very sensitive to the injected spectral index δ for $3 < \delta < 5$.

Values of the scale height s_0 greater than $\sim 3 \times 10^8$ cm did not lead to rapid enough spectral softening to be consistent with the observations. Once s_0 is reduced much below this value the degree of spectral softening remains essentially unchanged because the electrons are stopped rapidly compared to the 128 ms integration time.

In general, the larger s_t is, the higher the degree of spectral softening. This is because the faster electrons can become more spread out from the slower electrons before they reach the exponentially increasing density region. Values of s_t smaller than $\sim 5 \times 10^8$ cm did not lead to sufficiently rapid spectral softening. Thus the coronal loop length must be longer than this, which excludes the possibility of acceleration occurring close to or below the transition region. We therefore have for the density profile parameters the following constraints: $s_0 < 3 \times 10^8$ cm and $s_t > 5 \times 10^8$ cm.

The value of the injection width t_0 has a large effect on the spectral evolution. The larger the value of t_0, the smaller the amount of spectral softening because new particles are still being injected as the earlier particles reach the higher density regions. Small values of t_0 ($\lesssim .1$ s) lead to very rapid spectral softening and rapid decay of the burst. With the assumption of small pitch angles, injection widths $t_0 \lesssim .1$ s are incompatible with observations. If the injection width is less than $\sim .1$ s then large pitch angle electrons ($\sin^{-1} \alpha \gtrsim 30°$) are needed to spread the pulse out before it reaches the high density region ($s > s_t$). On the other hand, $t_0 \gtrsim .1$ s leads to a burst decay which is too slow. Thus, this model requires $.1\,\text{s} \lesssim t_0 \lesssim .2\,\text{s}$.

Figure 4 compares the calculated spectra with the data at point D for values of these

parameters (t_0, s_0, and s_t) outside of the acceptable ranges. The other parameters were adjusted so that the calculated spectra fit the data at times A and B. As is evident, the calculated spectra at point D no longer fit the data.

IV. SUMMARY AND DISCUSSION

We have solved the kinetic equation for accelerated particles undergoing Coulomb collisions in a background magnetized plasma. For a homogeneous plasma we have found an exact analytic solution describing the evolution of the distribution of particles in energy and pitch angles (with respect to the magnetic field). For an inhomogenous plasma, analytic solutions are possible only for particles with small pitch angles (namely, beams collimated along the field lines). We then compared the bremsstrahlung x-ray spectrum from a short burst of accelerated electrons with the high temporal resolution hard x-ray solar flare spectra observed by HXRBS on SMM.

The observed softening with time of the x-ray spectra rules out the homogeneous solution, which means that electrons do not lose most of their energy in the uniform density coronal portion of the flaring loop. Most of the x-ray emission then occurs at the base of the loop below the transition region. Consequently, the decay time and the degree of spectral softening are primarily determined by the spread in arrival time of the electron beam at the base of the loop. The more the particles are spaced out when they reach the transition region, the longer the burst decay time; and the greater the spread in arrival times between high and low energy particles, the higher the degree of spectral softening. The particles are spread out by a combination of the time of flight difference from the acceleration region to the chromosphere, and the initial injection time width. The pitch

angle, the energy, and the distance from the acceleration region to the transition region determine the time of flight to the transition region. Since the effect of collisions in the corona is small, the time of flight over the distance s_t is $s_t/c\beta\mu$. The difference in time of flight between electrons of different energies is therefore proportional to s_t. Thus, smaller s_t leads to less spectral softening . Therefore, injection of the accelerated particles near or below the transition region is ruled out for such bursts.

Furthermore, the larger the range of pitch angles, the smaller the injection time t_0 has to be in order to reproduce the observations. The small pitch angle assumption basically amounts to ignoring the difference in path length between particles of different pitch angles. Thus the time of flight difference from the acceleration region to the thick target is determined solely by the difference in particle energies. This is why our assumption of small pitch angle requires that t_0 be greater than .1 s. Otherwise, the decay of the burst would be too short. Kiplinger et al (1984) used the non-thermal beam model of Emslie (1983) to model the same burst. They assumed uniform pitch angle distribution over some range of pitch angles and a delta function in time input. Their model contains a range of large pitch angle electrons so it can accomodate a delta function in time input.

We have found that under the assumption that the pitch angles are small and that the injection distribution is seperable in time and energy, the flare parameters must satisfy the following constraints:

Flare Parameter	Constraint
injection time t_0	$.1\,\mathrm{s} < t_0 < .2\,\mathrm{s}$
electron spectral index δ	$4.1 < \delta < 4.5$
distance to transition region s_t	$s_t > 5 \times 10^8$ cm
column depth to transition region N_{tr}	$N_{tr} < 1.7 \times 10^{20}$ cm^{-2}
scale height below transition region s_0	$s_0 < 3 \times 10^8$ cm
B field convergence	$B_{tr}/B_{inj} < \alpha_0^{-2}$

Finally, we can make some order of magnitude arguments to show that injection times of this length are reasonable. Let the total burst energy in x-rays be E_x. If the burst energy is supplied by magnetic reconnection, then $E_x = (B^2/8\pi)VY\epsilon$. Here B is the magnitude of the magnetic field, and V is the volume of the accelerating region. The efficiency with which magnetic energy is converted into that of accelerated particles is ϵ and the efficiency with which the particle energy is converted into x-rays is Y. Typically Y is of the order 10^{-6} (Petrosian 1973). The acceleration timescale will be of order $t_0 \sim L/v_A$ where $L \sim V^{1/3}$ is the characteristic length of the acceleration region and $v_A = B/(4\pi\rho)^{1/2}$ is the Alfven velocity. For typical flare parameters, we find for the energy in x-rays

$$E_x \sim 10^{20} \left(\frac{B}{100\,\mathrm{Gauss}}\right)^5 \left(\frac{t_0}{.1\,\mathrm{s}}\right)^3 \left(\frac{n}{10^9\,\mathrm{cm}^{-3}}\right)^{-3/2} \epsilon\,\mathrm{ergs} \tag{36}$$

The observed energy in x-rays of the flare shown in figure 1 is of order 10^{19} ergs, in agreement with this order of magnitude estimate.

For a more exact analysis of the high time resolution observations, general solutions including spatial inhomogeneities and large pitch angles are needed. This will require

numerical solutions of the full equation. However, as shown by Leach and Petrosian (1983) and here for the homogeneous case, the small pitch angle solution is a good representation of the general solution and gives acceptable results to much larger pitch angle then expected.

Acknowledgements: We would like to thank Russell Hamilton and James McTiernan for helpful discussions. This work was supported by NASA grant 7092 and NSF grant ATM 8320439.

APPENDIX: SOLUTION OF THE INHOMOGENEOUS SMALL PITCH ANGLE EQUATION

We will solve equation (1) for the case where the electron pitch angle is small $\mu \approx 1$. First we will consider the case where $d\ln B/ds = 0$. From this solution, the solution with non-zero $d\ln B/ds$ follows immediately.

i) Uniform Magnetic Field: With a similar change of variables which led to equations (10) to (12), equation (25), valid for small pitch angles, can be written as

$$T\frac{\partial\tilde{\eta}}{\partial\rho}\frac{\partial\phi}{\partial t} + \beta\frac{\partial\tilde{\eta}}{\partial\rho}\frac{\partial\phi}{\partial\tau} - \frac{\partial\phi}{\partial\rho} = \frac{1}{\alpha}\frac{\partial}{\partial\alpha}(\alpha\frac{\partial\phi}{\partial\alpha}). \tag{A1}$$

Solutions to this equation take the form

$$\phi = \int_0^\infty e^{\omega^2\rho(\tilde{\eta})}\Psi(\omega, t, \tilde{\eta}, \tau)J_0(\omega\alpha)d\omega, \tag{A2}$$

where the function $\Psi(\omega, t, \tilde{\eta}, \tau)$ satisfies the equation

$$\frac{T}{\beta}\frac{\partial\Psi}{\partial t} + \frac{\partial\Psi}{\partial\tau} - \frac{\partial\Psi}{\partial\eta} = 0, \tag{A3}$$

and ϕ is now defined to be f/β. The variable η is defined such that

$$\frac{d\eta}{d\tilde{\eta}} \equiv \beta \tag{A4}$$

$$\eta = \int \beta^2 dE = \frac{E^2}{E+1} \tag{A5}$$

Defining new variables x and z

$$x \equiv \frac{1}{2}(\tau - \eta), \tag{A6}$$

$$z \equiv \frac{1}{2}(\tau + \eta), \tag{A7}$$

and using the chain rule

$$\frac{\partial}{\partial \tau} = \frac{1}{2}\frac{\partial}{\partial x} + \frac{1}{2}\frac{\partial}{\partial z}, \tag{A8}$$

$$\frac{\partial}{\partial \eta} = -\frac{1}{2}\frac{\partial}{\partial x} + \frac{1}{2}\frac{\partial}{\partial z}, \tag{A9}$$

equation (A3) becomes

$$\frac{T}{\beta}\frac{\partial \Psi}{\partial t} + \frac{\partial \Psi}{\partial x} = 0. \tag{A10}$$

Solutions to this equation take the general form

$$\Psi((x,z,t) = A\Big(t - \Omega(\eta,\tau)\Big)B(z) \tag{A11}$$

$$\Omega(\eta,\tau) \equiv \int_{c(z)}^{x} \frac{T(z+x')}{\beta(z-x')}dx', \tag{A12}$$

where the functions A, B, and c are determined by the initial conditions. The ω dependence of Ψ is suppressed here. We assume a separable initial distribution of electron flux injected at $\tau = 0$ of the form

$$F(\eta,\alpha,\tau=0,t) = g(\eta)h(\alpha)k(t) \tag{A13}$$

Noting that at $\tau = 0$, x and z are equal to $-\frac{1}{2}\eta$ and $\frac{1}{2}\eta$ respectively, from equations (A2), (A11), and (A12) we find

$$F(\tau=0) = \beta^2 \int_0^\infty e^{\omega^2 \rho(\eta)} A_\omega\Big(t - \Omega(\eta,\tau=0)\Big)B_\omega(\eta)J_0(\omega\alpha)d\omega \tag{A14}$$

$$\Omega(\eta,\tau=0) = \int_{c(\frac{1}{2}\eta)}^{-\frac{1}{2}\eta} \frac{T(\frac{1}{2}\eta+x')}{\beta(\frac{1}{2}\eta-x')}dx'. \tag{A15}$$

Next we multiply both sides by $J_0(\omega'\alpha)\alpha d\alpha$ and integrate over α using the relation

$$\int_0^\infty x J_0(\omega x)J_0(\omega' x)dx = \frac{1}{\omega}\delta(\omega-\omega'). \tag{A16}$$

Defining

$$H(\omega) \equiv \int_0^\infty J_0(\omega\alpha) h(\alpha) \alpha d\alpha, \tag{A17}$$

we then find

$$g(\eta)k(t)H(\omega) = e^{\omega^2 \rho(\eta)} A_\omega \Big(t - \Omega(\eta, \tau = 0)\Big) B_\omega(\eta). \tag{A18}$$

The function $\Omega(\eta, \tau = 0)$ must be equal to zero for the solution to be a product of a function of t and a function of η. For this integral to be zero for arbitrary functions $T(\tau)$, the limits of integration must be equal. Thus we can identify

$$c(\frac{1}{2}\eta) = -\frac{1}{2}\eta, \tag{A19}$$

$$B_\omega(\eta) = \frac{1}{\beta(\eta)} e^{-\omega^2 \rho(\eta)} g(\eta) H(\omega), \tag{A20}$$

$$A_\omega(t) = k(t), \tag{A21}$$

$$\Omega(\eta, \tau) = \int_{-z}^{x} \frac{T(z + x')}{\beta(z - x')} dx'. \tag{A22}$$

We can rewrite $\Omega(\eta, \tau)$ in a simpler form using the substitution

$$\tau' \equiv z + x', \tag{A23}$$

$$d\tau' = ds'/\lambda_0(s'), \tag{A24}$$

$$\Omega(\eta, \tau) = \int_{-z}^{x} \frac{T(z + x')}{\beta(z - x')} dx' = \int_0^s \frac{ds'}{c\beta(\eta + \tau - \tau(s'))}. \tag{A25}$$

Reintroducing the τ dependence, the flux distribution function becomes

$$F(E, \mu, \mathrm{s}, t) = \frac{\beta^2(\eta)}{\beta^2(\eta + \tau)} g(\eta + \tau) k\Big(t - \Omega(\eta, \tau)\Big) \int_0^\infty e^{-\omega^2[\rho(\eta+\tau) - \rho(\eta)]} H(\omega) J_0(\omega\alpha) \omega d\omega. \tag{A26}$$

Integrating this over $d\mu = \alpha d\alpha$ gives

$$W(E,\tau,t) \equiv \beta \int_{-1}^{1} f d\mu = \frac{\beta^2(\eta)}{\beta^2(\eta+\tau)} g(\eta+\tau) k\Big(t - \Omega(\eta,\tau)\Big) \qquad (A27)$$

where we have made use of equation (A16) with $\omega' = 0$.

ii) Non-uniform Magnetic Field: The integrated over pitch angle solution with varying magnetic field follows directly from this. Integrating equation (1) over all μ gives

$$\frac{\lambda_0}{c\beta^2}\frac{\partial W}{\partial t} + B(\tau)\frac{\partial}{\partial \tau}\left[\frac{1}{B(\tau)}\int_{-1}^{1} \mu f d\mu\right] = \frac{\partial}{\partial \eta}\left(\frac{W}{\beta^2}\right) \qquad (A28)$$

For small pitch angle we make the approximation

$$\int_{-1}^{1} \mu f d\mu \approx W(E,\tau,t)/\beta \qquad (A29)$$

which is correct to second order in α. We then find that $W/\beta B$ then satisfies the same differential equation as Ψ (equation A3).

$$\frac{T}{\beta}\frac{\partial (W/\beta B)}{\partial t} + \frac{\partial (W/\beta B)}{\partial \tau} - \frac{\partial (W/\beta B)}{\partial \eta} = 0 \qquad (A30)$$

We can then immediately write

$$W(E,\tau,t) = \frac{B(\tau)}{B(\tau=0)}\frac{\beta^2(\eta)}{\beta^2(\eta+\tau)} g(\eta+\tau) k\big(t - \Omega(\eta,\tau)\big) \qquad (A31)$$

References

Bai, T. and Ramaty, R., 1978, *Ap. J.*, **219**, 705.

Brown, J.C., 1973, *Solar Physics*, **31**, 143.

Emslie, A.G., 1983, *Ap. J.*, **271**, 367.

Kane, S.R. and Anderson, K.A., 1970, *Ap. J.*, **162**, 1003.

Kiplinger, A.L., Dennis, B.R., Emslie, A.G., Frost, K.J. and Orwig, L.E., 1983, *Ap. J. Letters*, **265**, L99.

Kiplinger, A.L., Dennis, B.R., Frost, K.J. and Orwig, K.J., 1984, *Ap. J. Letters*, **287**, L105.

Langer, S.H. and Petrosian, V., 1977, *Ap. J.*, **215**, 666.

Leach, J. and Petrosian, V., 1983, *Ap. J.*, **269**, 715.

Leach, J., 1984, Ph.D. Thesis, Stanford University, Stanford.

McTiernan, J.M.J. and Petrosian, V., 1987, in preparation, Stanford University, Stanford.

Petrosian, V., 1973, *Ap. J.*, **186**, 291.

Figure Captions

Figure 1: An example of a short timescale hard x-ray burst (27-496 keV) reported by Kiplinger et al (1984). The spectra at points 1 through 4 are given by the circles in figure 3.

Figure 2: Log$[G(k,t)/k]$ representing the expected bremsstrahlung spectrum vs photon energy k (equation 24) at different times for a homogeneous background. The injection spectrum is $k(t) = \exp(-t^2/t_0^2)$ and $g(E) \propto E^{-\delta}$. The injection width is $t_0 = .05\,\mathrm{s}$, the injected spectral index $\delta = 4.2$, and the background density is $10^{11}\ \mathrm{cm}^{-3}$. The curves from A to G represent the spectrum fro consecutive 128 ms time intervals. Note the spectral hardening with time.

Figure 3: Log$[G(k,t)/k]$ vs k equation (A27) integrated over τ at different times. The injection profile is given in equation (34) with $\delta = 4.2$, and $t_0 = .13\,\mathrm{s}$. The density profile is given in equation (35) with $n_0 = 10^{10}\ \mathrm{cm}^{-3}$, $s_0 = 10^7\ \mathrm{cm}$, and $s_t = 1.4 \times 10^9\ \mathrm{cm}$. Curves A through D are seperated in time by 128 ms and correspond to the points 1 through 4 on figure 1. The circles are the measured spectra from the HXRBS with $\pm 1\,\sigma$ uncertainties (from Kiplinger et al 1984).

Figure 4: The same as figure 3 except we show Graph D for values of t_0, s_t, and s_0 outside of the ranges specified in section IV showing how the graphs no longer match the observations. The remaining parameters (which turn out to be very close to those in figure 3) were chosen so that graphs A and B matched the observations.

i) $t_0 = .08\,\mathrm{s}$; ii) $t_0 = .22\,\mathrm{s}$; iii) $s_t = 3.5 \times 10^8\ \mathrm{cm}$; iv) $s_0 = 5 \times 10^8\ \mathrm{cm}$

Figure 1

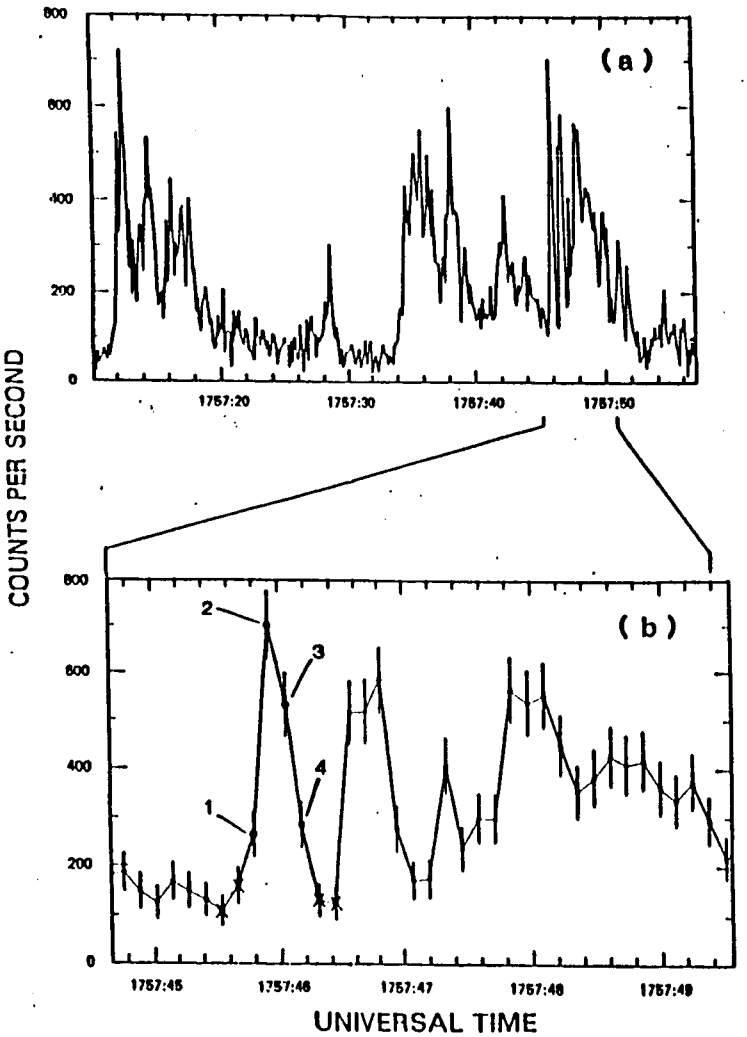

Figure 2

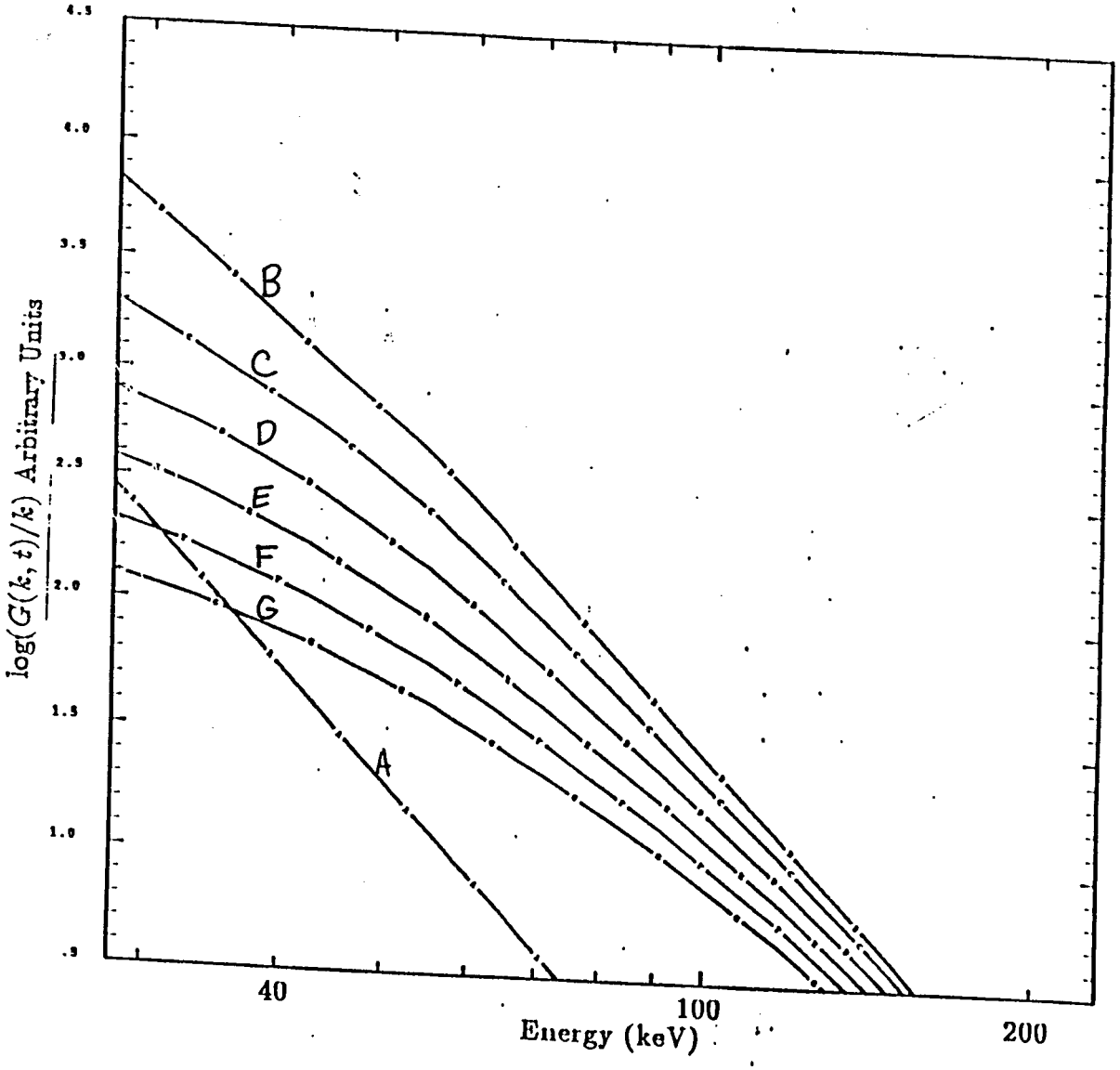

Figure 3

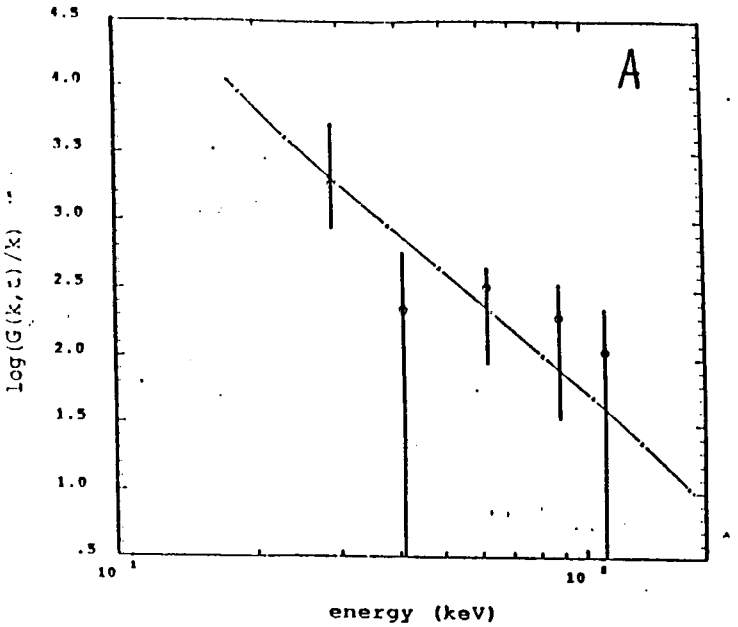

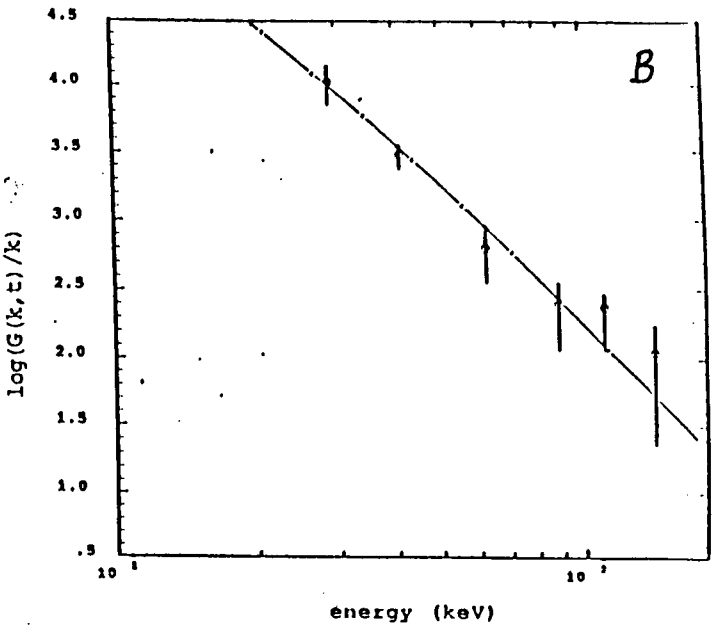

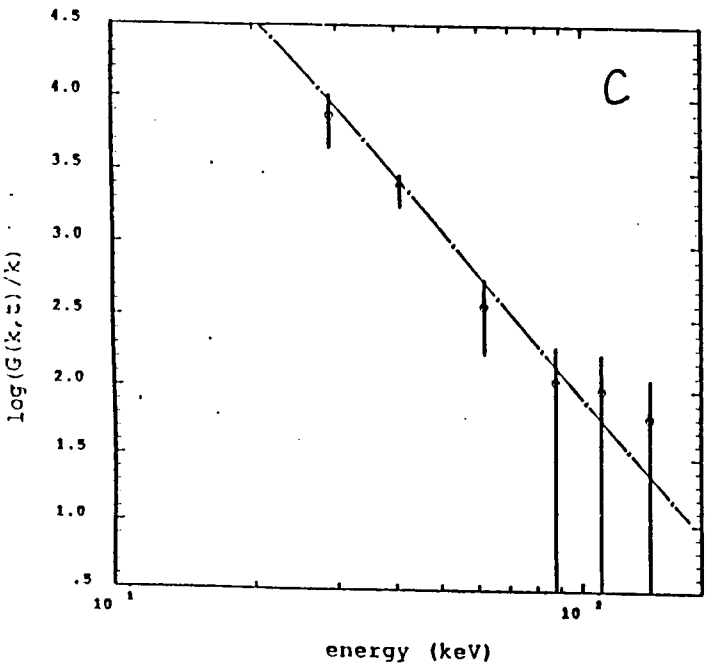

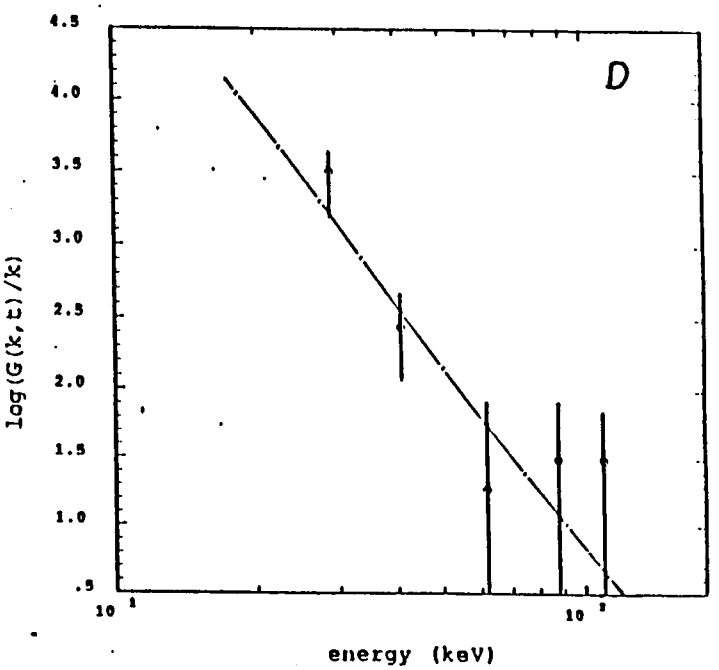

Figure 4